in vivo *36*: 2061-2073 (2022)
doi:10.21873/invivo.12932

The Role of mPGES-1 in Promoting Granulation Tissue Angiogenesis Through Regulatory T-cell Accumulation

TETSUYA HYODO[1,2,3], YOSHIYA ITO[1,2], KANAKO HOSONO[1,2], SATOSHI UEMATSU[4], SHIZUO AKIRA[5], MASATAKA MAJIMA[6], AKIRA TAKEDA[3] and HIDEKI AMANO[1,2]

[1]Department of Molecular Pharmacology, Graduate School of Medical Sciences, Kitasato University, Sagamihara, Japan;
Departments of [2]Pharmacology and [3]Plastic and Aesthetic Surgery, Kitasato University School of Medicine, Sagamihara, Japan;
[4]Department of Immunology and Genomics, Osaka City University Graduate School of Medicine, Osaka, Japan;
[5]Laboratory of Host Defense, WPI Immunology Frontier Research Center (IFReC), Osaka University, Osaka, Japan;
[6]Department of Medical Therapeutics, Kanagawa Institute of Technology, Atsugi, Japan

Abstract. *Background/Aim: Microsomal prostaglandin E synthase-1 (mPGES-1) is an enzyme, which catalyzes the final step of prostaglandin E_2 (PGE_2) synthesis. PGE_2 in involved in wound-induced angiogenesis. Regulatory T cells (Tregs) regulate not only immune tolerance but also tissue repair and angiogenesis. We examined whether the mPGES-1/PGE_2 axis contributes to wound-induced angiogenesis and granulation tissue formation through Treg accumulation. Materials and Methods: The dorsal subcutaneous tissues of male mPGES-1-deficient (mPGES-$1^{-/-}$) and C57BL/6 wild-type (WT) mice were implanted with polyurethane sponge disks. Angiogenesis was estimated by determining the wet weight of sponge tissues and the expression of proangiogenic factors including CD31, vascular endothelial growth factor (VEGF), and transforming growth factor β (TGF-β) in granulation tissues. Results: Angiogenesis was suppressed in mPGES-$1^{-/-}$ mice compared with WT mice, which was associated with attenuated forkhead box P3 (Foxp3) expression and $Foxp3^+$ Treg accumulation. The number of cells double-positive for Foxp3/TGFβ and Foxp3/VEGF were lower in mPGES-$1^{-/-}$ mice than in WT mice. Neutralizing Tregs with antibodies (Abs) against CD25 or folate receptor 4 (FR4) inhibited the Foxp3+ Treg angiogenesis and accumulation in WT mice, but not in mPGES-$1^{-/-}$ mice. The topical application of PGE_2 into the implanted sponge enhanced angiogenesis and accumulation of Tregs expressing TGFβ and VEGF in WT and mPGES-$1^{-/-}$ mice. Conclusion: Tregs producing TGFβ and VEGF accumulate in wounds and contribute to angiogenesis through mPGES-1-derived PGE_2. mPGES-1 induction may control angiogenesis in skin wounds by recruiting Tregs.*

Correspondence to: Hideki Amano, MD, Ph.D., Department of Pharmacology, Kitasato University School of Medicine, 1-15-1 Kitasato, Minami-ku, Sagamihara, Kanagawa 252-0374, Japan. Tel: +81 427788822, Fax: +81 427787604, e-mail: hideki@med.kitasato-u.ac.jp

Key Words: Tregs, angiogenesis, wound, mPGES-1, PGE_2.

The process of forming new blood vessels from the pre-existing vasculature is called angiogenesis. It takes place under physiological and pathological conditions including embryogenesis, inflammation, and cancer (1, 2). Thus, tissue repair from wounds and gastric ulcers depends on angiogenesis (3, 4). Various endogenous factors highly regulate the angiogenic process (5). Prostaglandins (PGs), including PGE_2, have been shown to stimulate angiogenesis (6) and PGs are synthesised by sequential actions of cyclooxygenase (COX) (COX-1 or COX-2) and the respective PGs synthases. We implanted a polyurethane sponge disk subcutaneously to elicit angiogenesis in the surrounding granulation tissues in rodents to analyse the mechanisms of angiogenesis *in vivo* (7, 8). Angiogenesis was reported to occur concomitantly with COX-2 induction, and to be inhibited by administration of selective COX-2 inhibitors (8, 9). Furthermore, COX-2-induced angiogenesis is associated with increased vascular endothelial growth factor (VEGF) expression, a main proangiogenic factor (8, 10). Microsomal PGE synthase-1 (mPGES-1) is an inducible enzyme that specifically catalyzes the synthesis of PGE_2 in inflammatory conditions. mPGES-1-deficient mice exhibit inflammatory granulation tissue formation attenuation and

angiogenesis (11). Moreover, mPGES-1 plays a role in angiogenesis during gastric ulcer healing in mice (3). These results suggest that PGE_2 derived from mPGES-1 mediates *in vivo* angiogenic action.

Regulatory T cells (Tregs) are known as the most important anti-inflammatory subset of T cells that mediate immune tolerance and tissue homeostasis (12). Tregs are characterized by the expression of the surface molecules CD4 and CD25 [the interleukin (IL)-2 cytokine receptor], and the forkhead box P3 (Foxp3) transcription factor (13). The role of Tregs in angiogenesis modulation has attracted increased attention (14, 15). Tregs proangiogenic action has been explored in various disease states, although mainly in oncology due to its powerful therapeutic potential. Furthermore, it has been shown that skin wound closure is delayed in Treg-depleted mice (16). In addition, the COX inhibitor aspirin has been shown to reduce angiogenesis and wound granulation formation in implanted sponge tissues, which was accompanied by reduced $Foxp3^+$ Treg cell recruitment in the granulation tissues (17).

Based on these results, we hypothesized that mPGES-1 promotes wound-induced angiogenesis and granulation tissue formation by inducing Tregs. Here we used a sponge implantation model to quantitatively evaluate angiogenesis to examine this possibility.

Materials and Methods

Animals. Male C57BL/6 WT mice (8 weeks old) were obtained from CLEA Japan (Tokyo, Japan). Male mPGES1$^{-/-}$ mice were previously described (18). Mice were maintained in a facility with constant humidity (50%±5%) and temperature (25˚C±1˚C) with a 12-h light/dark cycle and were provided with food and water *ad libitum*. All experimental procedures were approved by the Animal Experimentation and Ethics Committee of the Kitasato University School of Medicine (2020-107, 2021-83) and were performed following the animal experiment guidelines set by the Kitasato University School of Medicine in accordance with the "Guidelines for Proper Conduct of Animal Experiments" published by the Science Council in Japan.

Subcutaneous sponge implantation. Circular sponge disks (5-mm-thick and 15-mm- in diameter) were prepared from polyether polyurethane foam sheet (19). Sponge disks were implanted into dorsal subcutaneous tissues as described previously under anesthesia with an intraperitoneal (*i.p.*) injection of a combination cocktail containing 0.3 mg/kg of medetomidine hydrochloride (Nippon Zenyaku Kogyo, Fukushima, Japan), 4.0 mg/kg of midazolam (Astellas Pharma, Tokyo, Japan), and 5.0 mg/kg of butorphanol (Meiji Seika Pharma, Tokyo, Japan) (19). Medetomidine effects were reversed with the *i.p.* injection of atipamezole (Nippon Zenyaku Kogyo)-0.75 mg/kg post procedure.

Tissue sample preparation. Mice were euthanized with isoflurane at 7 or 14 days after surgery. The collected sponge granulation tissues were divided into two pieces: one was immediately fixed with 10% paraformaldehyde in 0.1-M phosphate-buffered solution (PBS; pH 7.4) and the other was immersed in TRIzol Reagent (Life Technologies, Grand Island, NY, USA) for isolating RNA to perform polymerase chain reaction (PCR) quantification.

Drugs. Prostaglandin E_2 (PGE_2; Cayman Chemicals, Ann Arbor, MI, USA) (30 nmol/50 μl/site) or vehicle (methyl acetate in PBS) was topically injected into the subcutaneously implanted sponges once a day under anesthesia with isoflurane the day after sponge implantation. In a separate experiment, a neutralizing Ab specific for the mouse folate receptor 4 (FR4) (50 μg per mouse, clone eBio TH6; eBioscience, San Diego, CA, USA) was *i.p.* injected on days 0, 3, 6, 9, and 12 after sponge disk implantation. Control animals were treated with isotype control IgG Abs (rat IgG2b, κ, BioLegend, San Diego, CA, USA). A group of mice received was injected *i.p.* with a neutralizing Ab for mouse CD25 (IL-2 receptor α chain) (250 μg per mouse, Bio X Cell Co., West Lebanon, NH, USA) dissolved in physiological saline, or the isotype-matched IgG (mouse IgG1, λ, BioLegend). They were administered at the day before the start of the mouse experiment and at 7 days after sponge disk implantation.

Histology and immunohistochemistry. Tissues were prepared as previously described (19). The sections were stained with hematoxylin and eosin (H&E) or processed for immunohistochemistry. For the latter, sections were stained with an anti-CD31 Ab (rabbit polyclonal; Abcam, Cambridge, MA, USA), transforming growth factor β (TGF-β) (Abcam), and Foxp3 (eBioscience). Immunoreactive signals were detected with 3,3'-diaminobenzidine, and specimens were counterstained with Mayer's hematoxylin or methyl green. A microscope (Biozero BZ-700 Series; Keyence, Osaka, Japan) was used to capture images of H&E- or immune-stained sections. Individual microvessels stained with CD31 Ab were counted in five high-power fields (×400). Microvessel density (MVD) was expressed as microvessel number per observed area (vessel number/field) (19).

Immunofluorescence analysis. Sections were prepared as described previously for immunofluorescence (19). The sections were incubated overnight at 4˚C using a rabbit anti-mouse mPGES-1 monoclonal Ab (Abcam), a rat anti-mouse CD68 Ab (Bio-Rad, Hercules, CA, USA), a rabbit anti-mouse TGF-β polyclonal Ab (Abcam), a goat anti-mouse VEGF polyclonal Ab (R&D Systems, Minneapolis, MN, USA), or a rat anti-mouse Foxp3 (eBioscience). Then, sections were incubated with a mixture of secondary antibodies for 1 h at room temperature: Alexa Fluor 594-conjugated donkey anti-rat IgG, Alexa Fluor 488-conjugated donkey anti-rabbit IgG, and Alexa Fluor 488-conjugated donkey anti-goat IgG were obtained from Molecular Probes (Eugene, OR, USA). A fluorescence microscope was used to capture the images (Biozero BZ-700; Keyence, Osaka, Japan). After labeling, five high-power optical fields (400× magnification) were randomly selected, and the number of positive cells was counted.

Quantitative real-time RT-PCR. Transcripts encoding mPGES-1, CD31, VEGF, TGFβ, Foxp3, and glyceraldehyde-3-phosphate dehydrogenase (GAPDH) were quantified by real-time RT-PCR analysis. TB Green Premix Ex TaqII (Tli RNaseH Plus; Takara Bio, Inc. Shiga, Japan) was used to perform quantitative PCR amplification. Gene-specific primers used for real-time RT-PCR were designed using the Primer 3 software based on GenBank data. The sequences of the primers were as follows: 5'-AGGATGCGCTG AAACGTGGAG-3' (sense) and 5'-CCGAGGAA-GAGGAAA GGATAG-3' (antisense) for mPGES-1; 5'-ACTTCTGAACTCC

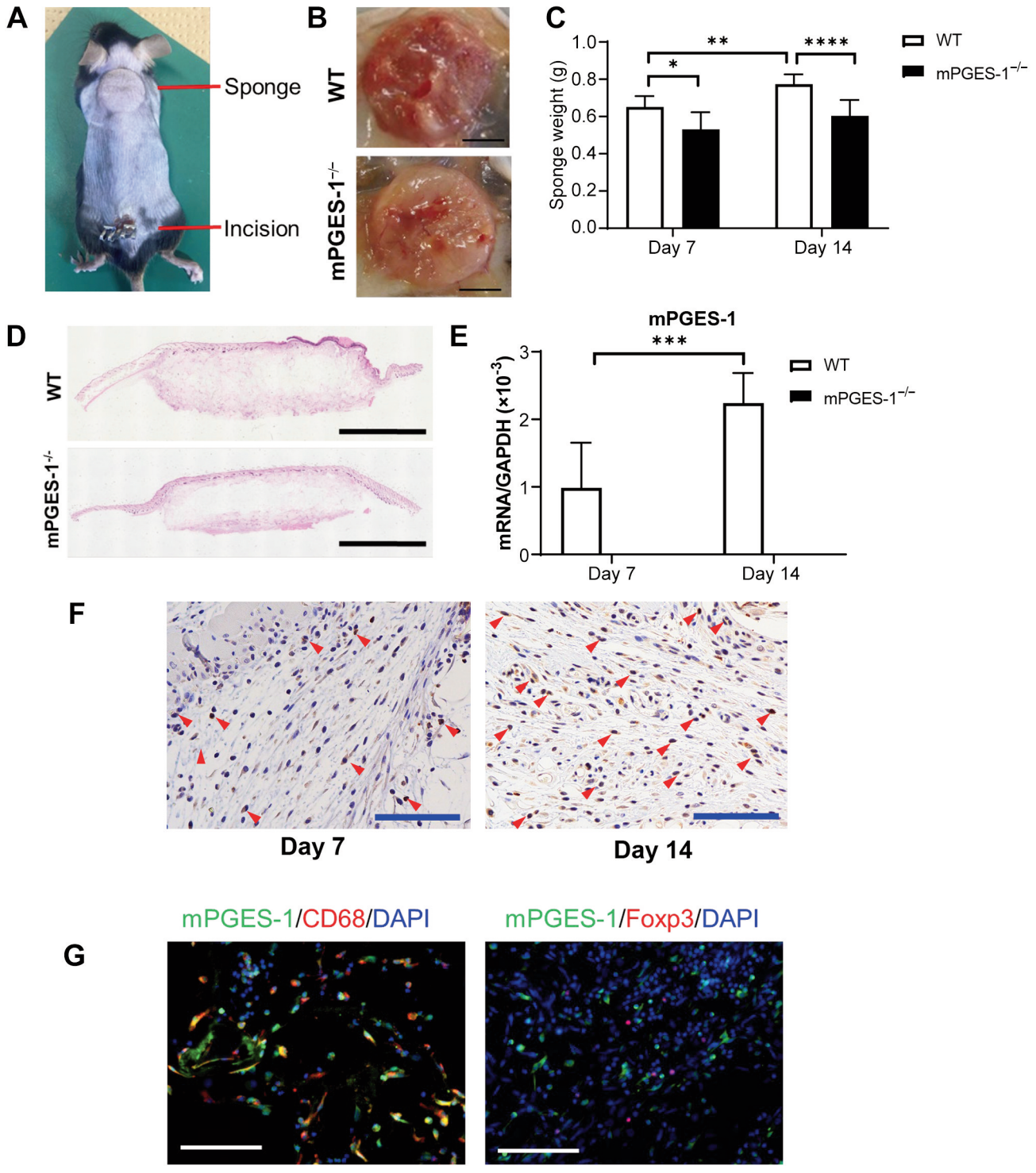

Figure 1. *Deficiency in mPGES-1 attenuates granulation tissue formation. (A) Typical appearance of the implanted sponge in subcutaneous tissues at the backs of mice. (B) Representative photos of sponge implants on day 14 removed from WT and mPGES-1$^{-/-}$ mice. Scale bars, 5 mm. (C) The sponge weight of WT and mPGES-1$^{-/-}$ mice on days 7 and 14. Data are expressed as mean±SD (n=8-10 mice per group). *p<0.05, **p<0.01, and ****p<0.0001. (D) Representative photomicrographs of sponge granulation tissue sections of WT and mPGES-1$^{-/-}$ mice on day 14. Scale bars, 5 mm. (E) Expression of mRNA encoding mPGES-1 in granulation tissue from WT and mPGES-1$^{-/-}$ mice on days 7 and 14. Data are expressed as mean±SD (6 mice per group). ***p<0.001. (F) Immunohistochemical staining for mPGES-1 in granulation tissues from WT mice on days 7 and 14. Scale bar, 100 μm. Red arrowheads indicate mPGES-1^{+} cells. (G) Double immunofluorescence staining for mPGES-1 (green)/CD68 (red) or Foxp3 (red) in granulation tissues from WT mice on day 7. Scale bars, 100 μm.*

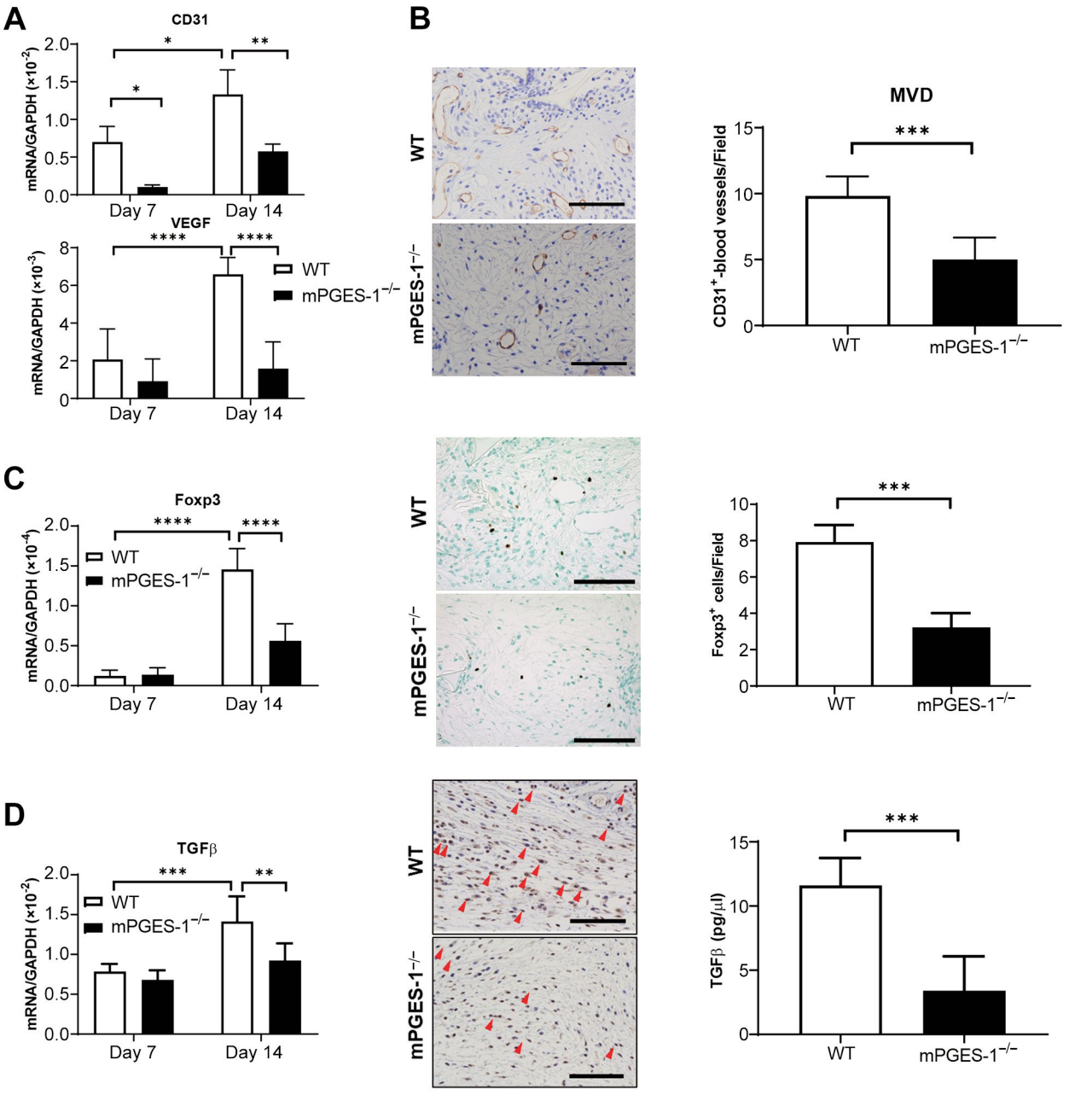

Figure 2. *Continued*

AACAGCGA-3' (sense) and 5'-CCATGTTCTG GGGGTCTTTAT-30 (antisense) for CD31; 5'-GAGAGAGGCCGAAGTCCTTT-3' (sense) and 5'-TTGGAACCGG-CATCTTTATC-3' (antisense) for VEGF; 5'-AACAATTCCTGGCGTTACCTT-3' (sense) and 5'-TGTATTCCGTCTCCTTGGTTC-3' (antisense) for TGFβ;5'-AGTGCCTGTGTCCTCAATGGTC-3' (sense) and 5'-AGGGCCA GCATAGGTGCAAG-3' (antisense) for Foxp3; 5'-ACATCA AGAAGGTGGTGAAGC-3' (sense) and 5'-AAGGTGGAAGA GTGGGAGTTG-3' (antisense) for GAPDH. Data were normalized to GAPDH expression levels.

Enzyme-linked immunosorbent assay (ELISA). Exudates in the dissected sponge granulation tissues were sampled with a 1-ml syringe after weighing the sponge granulation tissues The TGFβ concentration in exudates was measured using an ELISA kit (R&D).

Statistical analysis. All results are expressed as mean±standard deviation (SD). The GraphPad Prism software version 8 (GraphPad Software, La Jolla, CA, USA) was used to perform all statistical analyses. Data were compared between the two groups using unpaired two-tailed Student's *t*-tests and between multiple groups

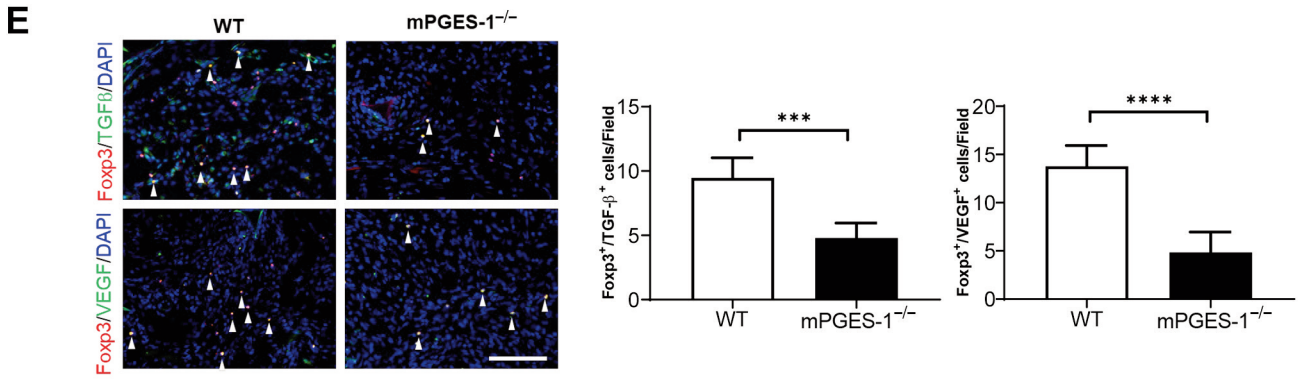

Figure 2. *Reduced Foxp3 angiogenesis and expression in granulation tissue in mPGES-1$^{-/-}$ mice. (A) The levels of mRNA encoding CD31 and VEGF in granulation tissues from WT and mPGES-1$^{-/-}$ mice on day 14. Data are expressed as mean±SD (n=6 mice per group). *p<0.05, **p<0.01, and ****p<0.0001. (B) Immunostaining for CD31 in granulation tissue. Scale bars, 100 μm. Microvessel density (MVD) in sponge granulation tissues from WT and mPGES-1$^{-/-}$ mice on day 14. Density was determined by CD31 immunostaining. Data are expressed as mean±SD (n=6 mice per group). ***p<0.001. (C) (left panel) Expression of mRNA encoding Foxp3 in the granulation tissue from WT and mPGES-1$^{-/-}$ mice on days 7 and 14. Data are expressed as mean±SD (n=6 mice per group). ****p<0.0001. (middle panels) Immunostaining for Foxp3 in granulation tissue from WT and mPGES-1$^{-/-}$ mice on day 14. Dark brown-stained cells indicate Foxp3^{+} cells. Scale bars, 100 μm. (right panel) Foxp3^{+} cells number in granulation tissue on day 14. Data are expressed as mean±SD (n=6 mice per group). ***p<0.001. (D) (left panel) Expression of mRNA encoding TGF-β in granulation tissue from WT and mPGES-1$^{-/-}$ mice on days 7 and 14. Data are expressed as mean±SD (n=6 mice per group). **p<0.01, ***p<0.001. (middle panels) TGF-β immunostaining in the granulation tissue surrounding sponge implants. Red arrowheads indicate TGF-β^{+} cells. Scale bars, 100 μm. (right panel) The TGFβ concentration in sponge implant exudates from WT and mPGES-1$^{-/-}$ mice on day 14. Data are expressed as mean±SD (n=6 mice per group). ***p<0.001. (E) (left panels) Double Foxp3 immunofluorescence staining (red)/TGFβ (green) or VEGF (green) in the granulation tissue from WT and mPGES-1$^{-/-}$ mice on day 14. White arrowheads indicate double-positive cells. Scale bars, 100 μm. (right panels) The numbers of cells double-positive for Foxp3/TGFβ and Foxp3/VEGF in granulation tissues from WT and mPGES-1$^{-/-}$ mice on day 14. Data are expressed as mean±SD (n=6 mice per group). ***p<0.001 and ****p<0.0001.*

using one-way analyses of variance followed by Tukey's post hoc tests. A p-value of <0.05 was considered statistically significant. Significance is depicted with asterisks on graphs: *p<0.05, **p<0.01, ***p<0.001, and ****p<0.0001.

Results

Suppression of granulation tissue formation in mPGES-1$^{-/-}$ mice. To elucidate the role of mPGES-1 in granulation tissue formation, sponge disks were implanted (Figure 1A). Formation of thick granulation tissues were observed around the sponge in WT mice on day 14 following implantation, whereas thin granulation tissues were found in mPGES-1$^{-/-}$ mice (Figure 1B). In WT mice, the sponge weight was progressively increased after sponge implantation. In addition, the weight of sponges in WT mice on days 7 and 14 was significantly heavier than that in mPGES-1$^{-/-}$ mice (Figure 1C). Granulation tissue formation was evaluated by histological examination (Figure 1D). Histological analysis of sponge tissues demonstrated that the granulation tissue area was lower in mPGES-1$^{-/-}$ mice than in WT mice (Figure 1D). These results suggest that mPGES-1 is involved in granulation tissue formation.

Next, we determined mPGES-1 expression in sponge granulation tissue (Figure 1E). mPGES-1 mRNA levels in WT mice were increased after sponge implantation. mPGES-1 expression was eliminated in mPGES-1$^{-/-}$ mice as expected. We evaluated mPGES-1 expression in granulation tissue of WT mice through immunohistochemical analysis (Figure 1F). Immunohistological analysis showed that several mPGES-1^{+} cells were present in granulation tissues. Furthermore, mPGES-1 was expressed in accumulated inflammatory-like cells in the granulation tissues of WT mice. Double immunofluorescence also demonstrated that mPGES-1 was expressed in CD68^{+} cells, indicating that macrophages expressed mPGES-1 (Figure 1G). mPGES-1 was not co-localized with Foxp3, although Foxp3^{+} cells were found at reduced rates compared to those of CD68^{+} cells (Figure 1G).

Angiogenesis reduction and Treg-cell accumulation in mPGES-1$^{-/-}$ mice. We also examined angiogenesis based on CD31 (an endothelial cell marker) expression since angiogenesis is necessary for the formation of wound granulation tissue. Real-time RT-PCR analysis revealed lower CD31 mRNA levels in mPGES-1$^{-/-}$ mice than in WT mice on day 14 (Figure 2A). The same was true for the mRNA expression of VEGF (Figure 2A). Angiogenesis was also evaluated by quantifying blood vessel lumen formation with CD31 immunostaining. Immunostaining analysis

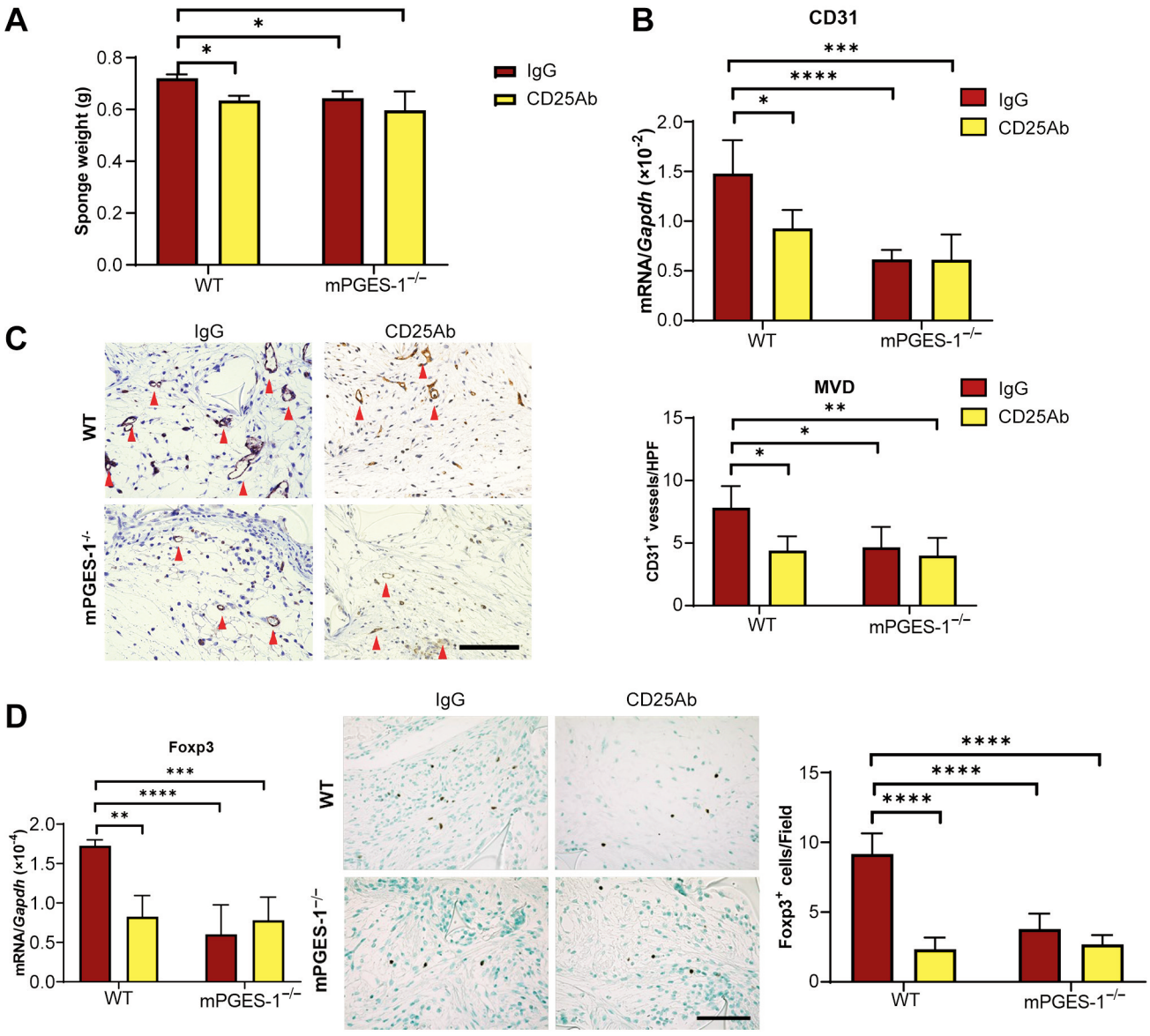

Figure 3. *Continued*

revealed that the number of $CD31^+$ vessels was lower in mPGES-$1^{-/-}$ mice than in WT mice (Figure 2B). Quantitative analysis revealed that MVD was lower in mPGES-$1^{-/-}$ mice than in WT mice (Figure 2B).

mRNA levels of Foxp3 were also determined since Tregs are involved in angiogenesis. Foxp3 expression was upregulated in WT mice on days 7 and 14 and were higher than those in mPGES-$1^{-/-}$ mice (Figure 2C). Immunohistochemical analysis showed that the number of $Foxp3^+$ cells was higher in WT mice than in mPGES-$1^{-/-}$ mice (Figure 2C), suggesting that mPGES-1 is involved in recruiting granulation tissue Tregs. We also determined TGF-β mRNA levels in the granulation tissues since TGFβ is a potent angiogenesis-stimulating factor (20), which were found to be lower in mPGES-$1^{-/-}$ mice than in WT mice (Figure 2D). TGF-β expression in the granulation tissues of mPGES-$1^{-/-}$ mice was lower than that of WT mice as demonstrated in immunohistology. TGF-β concentration in exudates in the implanted sponge disks in mPGES-$1^{-/-}$ mice were lower compared with that in WT mice (Figure 2D). Immunofluorescence showed that TGF-β or VEGF expression was co-localized with $Foxp3^+$ cells (Figure 2E). The numbers of $Foxp3^+/TGF\beta^+$ and $Foxp3^+/VEGF^+$ cells in the granulation tissues were lower in mPGES-$1^{-/-}$ mice than

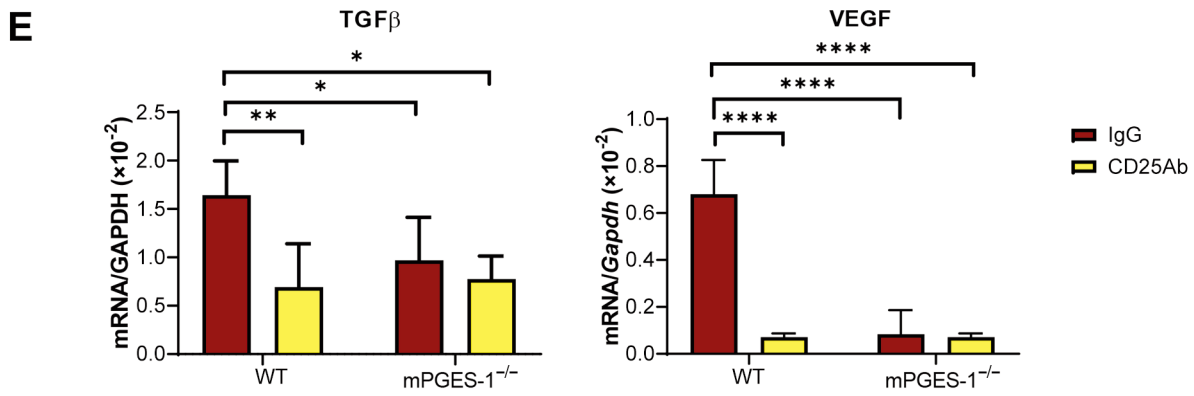

Figure 3. *Neutralizing antibody effects against CD25 on granulation tissue formation and angiogenesis in WT and mPGES-1$^{-/-}$ mice. (A) The sponge weight on day 14 in WT and mPGES-1$^{-/-}$ mice treated with CD25 antibody (Ab) or control IgG. Data are expressed as mean±SD (n=4-6 mice per group). *p<0.05, **p<0.01. (B) CD31 mRNA expression in WT and mPGES-1$^{-/-}$ mice treated with CD25 Ab or control IgG. Data are expressed as mean±SD (n=4-6 mice per group). *p<0.05, ***p<0.001, and ****p<0.0001. (C) (left panels) Immunostaining for CD31 in granulation tissue surrounding sponge implants. Scale bars, 100 μm. (right panel) MVD in sponge granulation tissues on day 14 from WT and mPGES-1$^{-/-}$ mice treated with CD25 Ab or control IgG. Density was determined by CD31 immunostaining. Data are expressed as mean±SD (n=4-6 mice per group). *p<0.05, **p<0.01. (D) (left panel) Expression of mRNA encoding Foxp3 in granulation tissue from WT and mPGES-1$^{-/-}$ mice treated with CD25 Ab or control IgG on day 14. Data are expressed as mean±SD (n=4-6 mice per group). **p<0.01, ***p<0.001, and ****p<0.0001. (middle panels) Immunostaining for Foxp3 in granulation tissue surrounding the sponge implants on day 14. Dark brown-stained cells indicate Foxp3^{+} cells. Scale bars, 100 μm. (right panel) Foxp3^{+} cell numbers in granulation tissues on day 14. Data are expressed as mean±SD (n=4-6 mice per group). ****p<0.0001. (E) Expression of mRNA encoding TGF-β and VEGF in granulation tissue from WT and mPGES-1$^{-/-}$ mice treated with CD25 Ab or control IgG on day 14. Data are expressed as mean±SD (n=4-6 mice per group). *p<0.05, **p<0.01, and ****p<0.0001.*

in WT mice (Figure 2E). Collectively, the formation of granulation tissues after sponge implantation was associated with Treg accumulation and TGF-β and VEGF expression enhancements.

Decreased Tregs impaired angiogenesis and formation of granulation tissues. We examined whether Tregs contributed to granulation tissue formation and angiogenesis by depleting Tregs in WT and mPGES-1$^{-/-}$ mice using anti-CD25 or anti-FR4 Ab. Treatment of WT mice with CD25 Ab significantly decreased the sponge weights on day 14 as compared with control IgG-treated WT mice (Figure 3A). Conversely, no statistically significant difference was observed in sponge weights between the two treatments in mPGES-1$^{-/-}$ mice. Angiogenesis was attenuated in CD25 Ab-treated WT mice as indicated by CD31 mRNA (Figure 3B) and protein expression (Figure 3C) and MVD, and as compared with the control IgG-treated WT mice. However, CD25 Ab treatment of mPGES-1$^{-/-}$ mice did not further affect the reduced angiogenesis in the controls. The Foxp3 mRNA levels and Treg accumulation in the granulation tissue in WT mice but not in mPGES-1$^{-/-}$ mice decreased with CD25 Ab treatment (Figure 3D). Finally, TGF-β mRNA levels were lower in CD25 Ab-treated WT mice than in control IgG-treated WT mice. Reduced TGF-β levels in CD25 Ab-treated WT mice were similar to those in mPGES-1$^{-/-}$ mice treated with CD25 Ab or control IgG (Figure 3E). The same was true for the VEGF levels (Figure 3E). Our results suggest that Treg accumulation in granulation tissues is associated with enhanced angiogenesis and TGF-β and VEGF expression and this accumulation depends on mPGES-1.

In addition, the treatment of WT mice with anti-FR4 Ab decreased the sponge weight on day 14 compared to treatment with IgG treatment. There was, however, no statistically significant difference in the weight of mPGES-1$^{-/-}$ mice between the two treatments (Figure 4A). Angiogenesis, as indicated by CD31 mRNA levels and MVD, was attenuated in FR4 Ab-treated WT mice as compared with IgG-treated WT mice (Figure 4B and C). Foxp3 mRNA levels and the number of FoxP3^{+} cells in granulation tissues were lower in FR4 Ab-treated WT mice than in IgG-treated WT mice (Figure 4D). These were associated with decreased TGF-β and VEGF mRNA levels in FR4 Ab-treated WT mice (Figure 4E). There were no statistically significant differences in sponge weights in mPGES-1$^{-/-}$ mice, accumulation of Tregs, angiogenesis, and TGF-β and VEGF expression between the treatments with FR4 Ab and control IgG.

Angiogenesis enhancement in granulation tissues and Treg accumulation by PGE_2 injection. Lastly, we examined whether PGE_2 derived produced through the activity of mPGES-1 contributes to granulation tissue angiogenesis and Treg accumulation. A single PGE_2 dose topically injected into

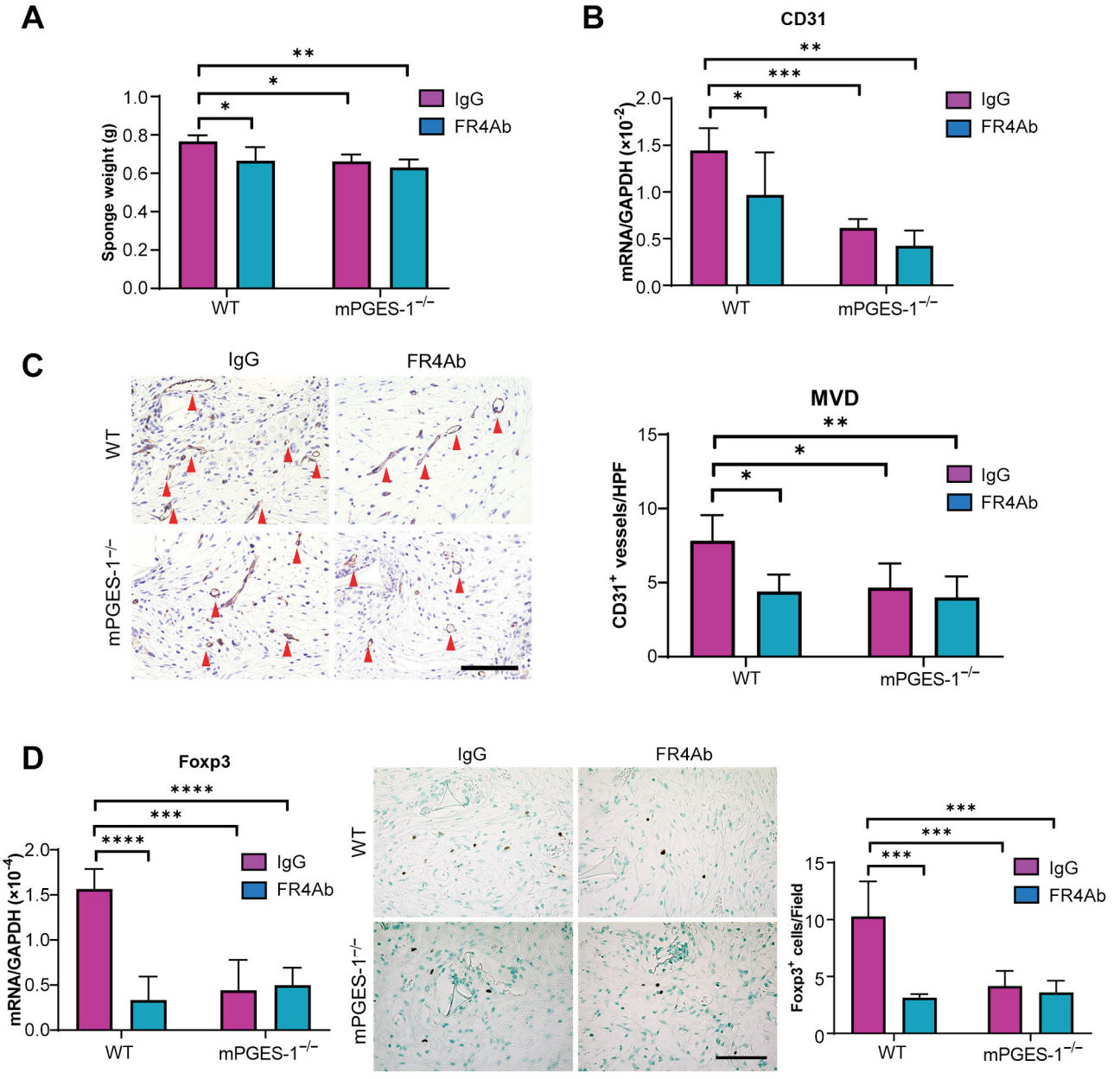

Figure 4. *Continued*

sponges in WT and mPGES-1$^{-/-}$ mice resulted in increase in sponge weights, angiogenesis as measured by CD31 mRNA expressions and blood vessel density, Treg accumulation, and TG-Fβ and VEGF expression levels in granulation tissues and in Foxp3^{+} Tregs, as compared with WT and mPGES-1$^{-/-}$ mice treated with the vehicle (Figure 5). These results indicated that PGE_2 enhanced granulation tissue angiogenesis and Treg accumulation in WT and mPGES-1$^{-/-}$ mice. These results suggested that mPGES-1-derived PGE_2 facilitates granulation tissue angiogenesis and Treg accumulation.

Discussion

We showed that mPGES-1 is involved in wound-induced angiogenesis and formation of wound granulation using a sponge implant model. Wound granulation angiogenesis was associated with Treg accumulation and TGFβ and VEGF expression enhancement. Treatment with neutralizing antibodies against CD25 or FR4 attenuated wound granulation formation, angiogenesis, and Treg accumulation in an mPGES-1-dependent manner. Topical PGE_2 application enhanced

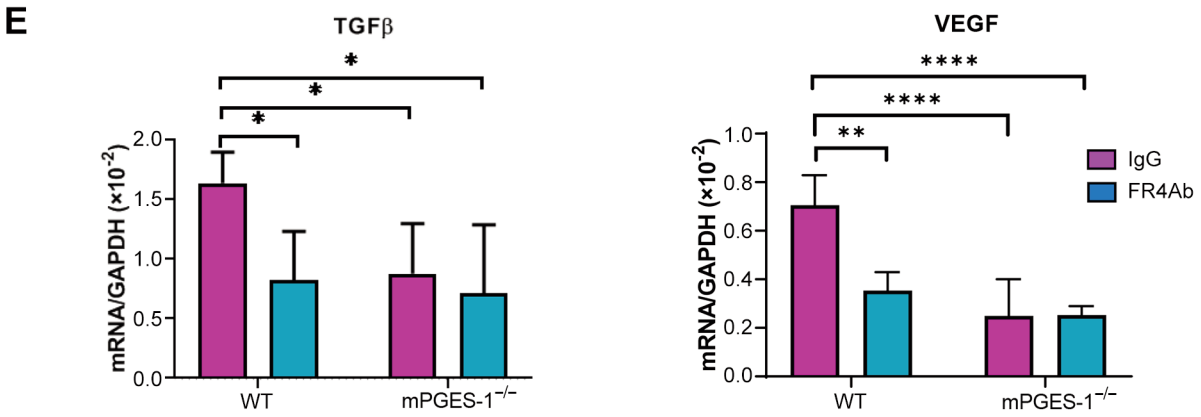

Figure 4. *Neutralizing antibody effects against FR4 on granulation tissue formation and angiogenesis in WT and mPGES-1$^{-/-}$ mice. (A) The sponge weight on day 14 in WT and mPGES-1$^{-/-}$ mice treated with FR4 Ab or control IgG. Data are expressed as mean±SD (n=4-6 mice per group). *p<0.05, **p<0.01. (B) CD31 mRNA expression in WT and mPGES-1$^{-/-}$ mice treated with FR4 Ab or control IgG. Data are expressed as mean±SD (n=4-6 mice per group). *p<0.05, **p<0.01, and ***p<0.001. (C) (left panels) Immunostaining for CD31 in granulation tissues surrounding sponge implants. Scale bars, 100 μm. (right panel) MVD in sponge granulation tissues on day 14 from WT and mPGES-1$^{-/-}$ mice with FR4 Ab or control IgG. Density was determined by CD31 immunostaining. Data are expressed as mean±SD (n=4-6 mice per group). *p<0.05, **p<0.01. (D) (left panel) Expression of mRNA encoding Foxp3 in granulation tissues from WT and mPGES-1$^{-/-}$ mice treated with FR4 Ab or control IgG on day 14. Data are expressed as mean±SD (n=4-6 mice per group). ***p<0.001 and ****p<0.0001. (middle panels) Immunostaining for Foxp3 in granulation tissues surrounding sponge implants on day 14. Dark brown-stained cells indicate Foxp3^{+} cells. Scale bars, 100 μm. (right panel) Foxp3^{+} cells number in granulation tissues on day 14. Data are expressed as mean±SD (n=4-6 mice per group). ***p<0.001. (E) Expression of mRNA encoding TGFβ and VEGF in granulation tissues from WT and mPGES-1$^{-/-}$ mice treated with FR4 Ab or control IgG on day 14. Data are expressed as mean±SD (n=4-6 mice per group). *p<0.05, **p<0.01, and ****p<0.0001.*

granulation tissue angiogenesis and Treg accumulation in WT and mPGES-1$^{-/-}$ mice.

Angiogenesis is indispensable during the process of wound granulation tissue formation. Eicosanoids play an important role in wound-induced angiogenesis (21). Among them, PGE_2 is an important player for angiogenesis during skin wound healing (21). Additionally, we have shown that PGE_2 has proangiogenic activity in wound healing (6, 22). A surgical sponge model was used to evaluate angiogenesis during the wound healing processes (4, 9, 10, 19). Increased angiogenesis in sponge granulation tissues was associated with increased mPGES-1 expression in this study, which is an inducible enzyme that mediates production of PGE_2 generation at the inflammation sites (23). By contrast, mPGES-1$^{-/-}$ mice showed attenuated angiogenesis and granulation tissue development. Reduced mPGES-1 expression may be closely associated with reduced PGE_2 levels in sponge granulation tissues. The present results revealed that PGE_2 injection in the sponge promoted angiogenesis in WT mice, which was consistent with our previous results (9, 22). Furthermore, exogenous administration of PGE_2 to mPGES-1$^{-/-}$ mice improved angiogenesis. Collectively, these results suggest that mPGES-1-derived PGE_2 is involved in angiogenesis and granulation tissue formation.

The current study showed that macrophages recruited into granulation tissues express mPGES-1. This suggests that macrophages produce PGE_2 by inducing mPGES-1. Consistent with this, PGE_2 released from immigrating macrophages helps promote wound healing (24, 25). Moreover, mPGES-1-derived PGE_2 in macrophages was also found to contribute to the angiogenesis and tissue repair from gastric ulcers and hepatic ischemia/reperfusion injury (3, 26). Accumulating evidence indicates that Tregs play a role in angiogenesis in addition to macrophages recruited to granulation tissues for wound healing (15). Tregs expressing VEGFR-1^{+}CXCR4^{+}Foxp3^{+} also contribute to angiogenesis and mucosal healing after a chemical-induced acute colitis (27). In addition, neutralizing antibodies against CD25 suppress angiogenesis in sponge-induced granulation tissues (17), which is in agreement with our present results. This study further confirmed this through Treg depletion with neutralizing antibodies against FR4, demonstrating that FR4 treatment antibodies inhibited angiogenesis. These suggest that Tregs play a role in wound-induced angiogenesis. Our data also indicate that the involvement of Tregs in wound-induced angiogenesis depends on the mPGES-1/PGE_2 axis. The association between high Treg levels and microvessel density has been reported in cancer models (15).

The results of this study suggested that Tregs facilitate wound-induced angiogenesis by upregulating VEGF in an mPGES-1-dependent manner. During the process of granulation tissue formation in response to sponge implants,

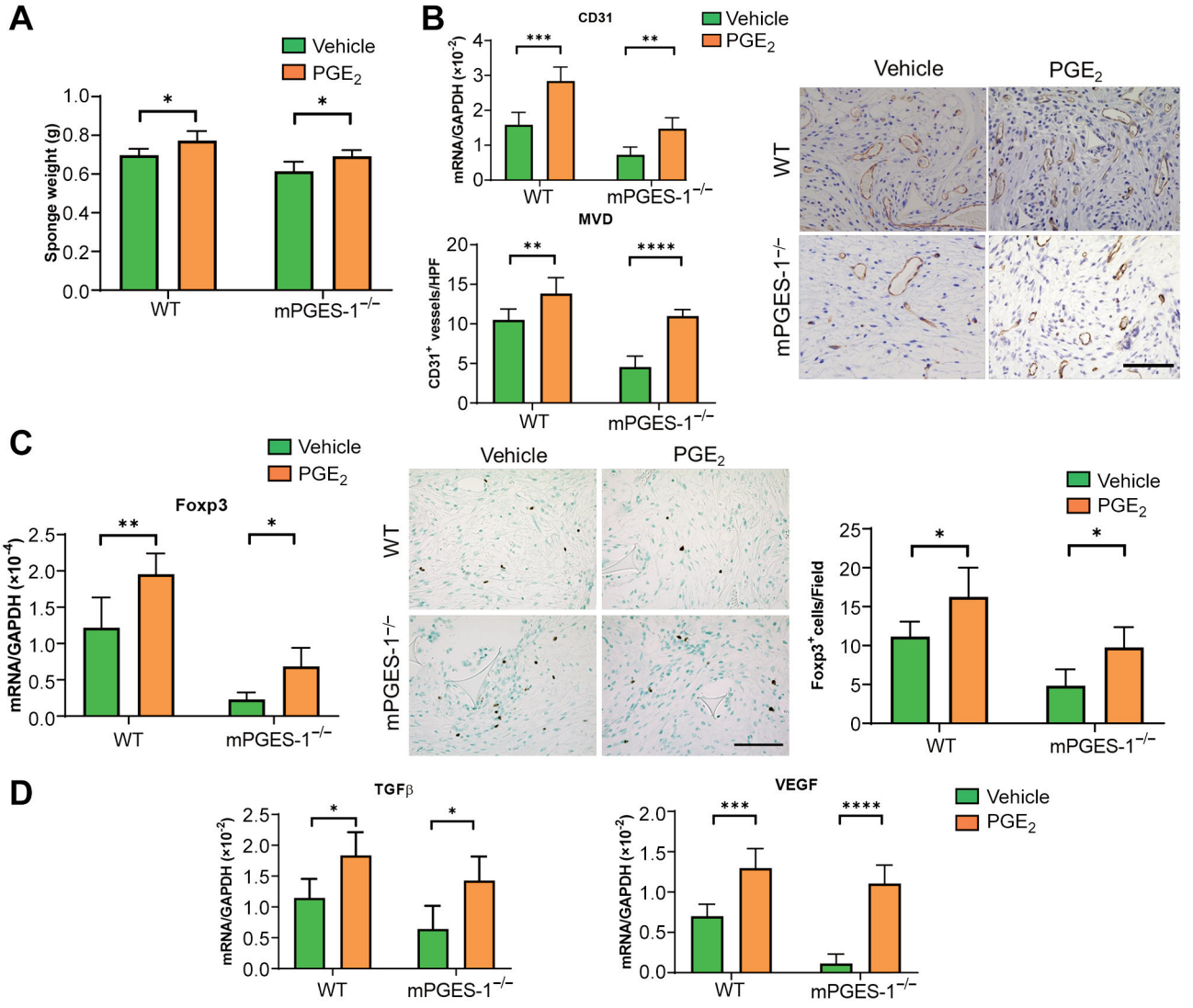

Figure 5. *Continued*

COX-2/PGE_2-induced angiogenesis was associated with upregulation of VEGF expression (9, 10, 19, 22).

Our data further demonstrated that PGE_2 injection enhanced VEGF expression in granulation tissues from WT and mPGES-$1^{-/-}$ mice, which was associated with enhanced angiogenesis. Neutralizing antibodies against VEGF suppress angiogenesis in sponge granulation tissues (17, 19). Collectively, these results indicate that endogenous mPGES-1 contributes to wound-induced angiogenesis by producing VEGF. Treg accumulation is correlated with VEGF expression in the tumor environment, which is consistent with this (28). Tregs promote angiogenesis directly by upregulating VEGF levels (29). An association between FOXP3 and VEGF gene expression and intratumoral microvessel density has been reported (30).

Although VEGF is the main proangiogenic factor, several other proangiogenic factors such as TGF-β also facilitate wound-induced angiogenesis (20). In this study, Tregs recruited to the wound granulation tissues appeared to produce TGF-β that induces angiogenesis in an mPGES-1/PGE_2-dependent manner. We previously demonstrated that aspirin inhibits granulation tissue angiogenesis, which is associated with decreased Treg accumulation together with TGF-β expression (17). Moreover, we have shown that TGF-β induces angiogenesis during the wound healing process (31). Furthermore, Tregs recruited into the endometriotic tissue produce TGF-β (32).

Collectively, Tregs enhance wound-induced angiogenesis by upregulating proangiogenic factors, including VEGF and TGF-β. However, the underlying mechanisms by which Treg

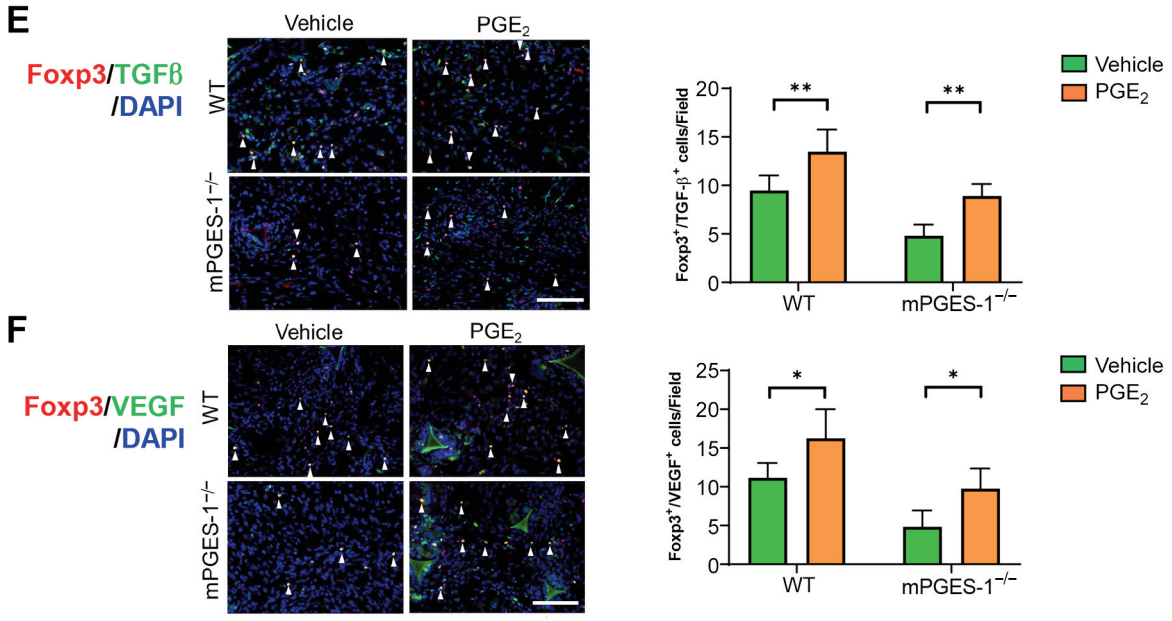

Figure 5. *Topical PGE_2 application enhances wound granulation formation and angiogenesis on day 14 in WT and mPGES-1$^{-/-}$ mice. (A) The sponge weight in WT and mPGES-1$^{-/-}$ mice treated with vehicle or PGE_2. Data are expressed as mean±SD (n=5-6 mice per group). *p<0.05. (B) Expression of mRNA encoding CD31 in granulation tissues from WT and mPGES-1$^{-/-}$ mice. Data are expressed as mean±SD (n=4-6 mice per group). **p<0.01, ***p<0.001. MVD in granulation tissue from WT and mPGES-1$^{-/-}$ mice treated with vehicle or PGE_2. Density was determined by CD31 immunostaining. Data are expressed as mean±SD (n=6 mice per group). **p<0.01, ****p<0.0001. CD31 immunostaining in granulation tissues surrounding sponge implants. Scale bars, 100 μm. (C) Expression of mRNA encoding Foxp3 in granulation tissues from WT and mPGES-1$^{-/-}$ mice. Data are expressed as mean±SD (n=4-6 mice per group). *p<0.05, **p<0.01. Immunostaining for Foxp3 in granulation tissues from WT and mPGES-1$^{-/-}$ mice treated with vehicle or PGE_2. Dark brown-stained cells indicate Foxp3$^+$ cells. Scale bars, 100 μm. Foxp3$^+$ cells number in granulation tissues. Data are expressed as mean±SD (n=6 mice per group). *p<0.05. (D) Expression of mRNA encoding TGF-β and VEGF in granulation tissue from WT and mPGES-1$^{-/-}$ mice. Data are expressed as mean±SD (n=4-6 mice per group). *p<0.05, ***p<0.001, ****p<0.0001. (E) Foxp3 double immunofluorescence staining (red)/TGF-β (green) in granulation tissues from WT and mPGES-1$^{-/-}$ mice treated with vehicle or PGE_2. White arrowheads indicate double-positive cells. Scale bars, 100 μm. Double-positive cell numbers for Foxp3/TGF-β. Data are expressed as mean±SD (n=6 mice per group). **p<0.01. (F) Foxp3 (red)/VEGF (green) double immunofluorescence staining in granulation tissues from WT and mPGES-1$^{-/-}$ mice treated with vehicle or PGE_2. White arrowheads indicate double-positive cells. Scale bars, 100 μm. Double-positive cell numbers for Foxp3/VEGF. Data are expressed as mean±SD (n=5-6 mice per group). **p<0.01.*

cells regulate VEGF and TGF-β signaling remain unclear.

Tregs are recruited into cancer or endometriotic tissue during cancer growth and endometriosis by upregulating chemokines including C–C motif chemokine ligand (CCL)28 (29) or CCL17 and CCL22 (32), respectively. Tregs appeared to have migrated from secondary lymphoid organs in the wounded skin, because the treatment with FTY720, which inhibits lymphocyte egress from the lymphoid organs, decreased Tregs at wound granulation tissue (16). Although this study indicated mPGES-1-dependent Treg accumulation into the wound granulation tissues, the underlying mechanisms by which Tregs are recruited in the wound tissue remain unexplored.

In conclusion, our data show that mPGES-1-derived PGE_2 facilitates wound-induced angiogenesis by producing TGFβ and VEGF in accumulated Tregs, resulting in wound granulation tissue formation. Induction of mPGES-1 may be a strategy for angiogenesis in skin wounds.

Conflicts of Interest

The Authors declare no conflicts of interest in relation to this study.

Authors' Contributions

Tetsuya Hyodo and Yoshiya Ito conceived, designed, performed the experiments, and wrote the manuscript. Kanako Hosono performed the experiments and contributed to immunofluorescence. Satoshi Uematsu and Shizuo Akira provided breeding of *mPges-1*$^{-/-}$ mice and helped to design the animal experiments. Masataka Majima and Akira Takeda verified the results of the experiments and provided critical advice to optimize the experimental protocols. Hideki Amano analyzed the data and revised the manuscript critically for intellectual content.

Acknowledgements

The Authors thank Michiko Ogino and Kyoko Yoshikawa for their technical assistance. This work was supported by grants from the

Japanese Ministry of Education, Culture, Sports, Science, and Technology (MEXT) (19K09250 and 22K08942 to HA).

References

1 Ferrara N, Gerber HP and LeCouter J: The biology of VEGF and its receptors. Nat Med *9(6)*: 669-676, 2003. PMID: 12778165. DOI: 10.1038/nm0603-669

2 Carmeliet P and Jain RK: Angiogenesis in cancer and other diseases. Nature *407(6801)*: 249-257, 2000. PMID: 11001068. DOI: 10.1038/35025220

3 Ae T, Ohno T, Hattori Y, Suzuki T, Hosono K, Minamino T, Sato T, Uematsu S, Akira S, Koizumi W and Majima M: Role of microsomal prostaglandin E synthase-1 in the facilitation of angiogenesis and the healing of gastric ulcers. Am J Physiol Gastrointest Liver Physiol *299(5)*: G1139-G1146, 2010. PMID: 20813913. DOI: 10.1152/ajpgi.00013.2010

4 Oba K, Hosono K, Amano H, Okizaki S, Ito Y, Shichiri M and Majima M: Downregulation of the proangiogenic prostaglandin E receptor EP3 and reduced angiogenesis in a mouse model of diabetes mellitus. Biomed Pharmacother *68(8)*: 1125-1133, 2014. PMID: 25465154. DOI: 10.1016/j.biopha.2014.10.022

5 Werner S and Grose R: Regulation of wound healing by growth factors and cytokines. Physiol Rev *83(3)*: 835-870, 2003. PMID: 12843410. DOI: 10.1152/physrev.2003.83.3.835

6 Majima M, Amano H and Hayashi I: Prostanoid receptor signaling relevant to tumor growth and angiogenesis. Trends Pharmacol Sci *24(10)*: 524-529, 2003. PMID: 14559404. DOI: 10.1016/j.tips.2003.08.005

7 Majima M, Isono M, Ikeda Y, Hayashi I, Hatanaka K, Harada Y, Katsumata O, Yamashina S, Katori M and Yamamoto S: Significant roles of inducible cyclooxygenase (COX)-2 in angiogenesis in rat sponge implants. Jpn J Pharmacol *75(2)*: 105-114, 1997. PMID: 9414024. DOI: 10.1254/jjp.75.105

8 Amano H, Haysahi I, Yoshida S, Yoshimura H and Majima M: Cyclooxygenase-2 and adenylate cyclase/protein kinase A signaling pathway enhances angiogenesis through induction of vascular endothelial growth factor in rat sponge implants. Hum Cell *15(1)*: 13-24, 2002. PMID: 12126060. DOI: 10.1111/j.1749-0774.2002.tb00095.x

9 Amano H, Hayashi I, Endo H, Kitasato H, Yamashina S, Maruyama T, Kobayashi M, Satoh K, Narita M, Sugimoto Y, Murata T, Yoshimura H, Narumiya S and Majima M: Host prostaglandin E(2)-EP3 signaling regulates tumor-associated angiogenesis and tumor growth. J Exp Med *197(2)*: 221-232, 2003. PMID: 12538661. DOI: 10.1084/jem.20021408

10 Majima M, Hayashi I, Muramatsu M, Katada J, Yamashina S and Katori M: Cyclo-oxygenase-2 enhances basic fibroblast growth factor-induced angiogenesis through induction of vascular endothelial growth factor in rat sponge implants. Br J Pharmacol *130(3)*: 641-649, 2000. PMID: 10821793. DOI: 10.1038/sj.bjp.0703327

11 Kamei D, Yamakawa K, Takegoshi Y, Mikami-Nakanishi M, Nakatani Y, Oh-Ishi S, Yasui H, Azuma Y, Hirasawa N, Ohuchi K, Kawaguchi H, Ishikawa Y, Ishii T, Uematsu S, Akira S, Murakami M and Kudo I: Reduced pain hypersensitivity and inflammation in mice lacking microsomal prostaglandin e synthase-1. J Biol Chem *279(32)*: 33684-33695, 2004. PMID: 15140897. DOI: 10.1074/jbc.M400199200

12 Sakaguchi S, Yamaguchi T, Nomura T and Ono M: Regulatory T cells and immune tolerance. Cell *133(5)*: 775-787, 2008. PMID: 18510923. DOI: 10.1016/j.cell.2008.05.009

13 Vignali DA, Collison LW and Workman CJ: How regulatory T cells work. Nat Rev Immunol *8(7)*: 523-532, 2008. PMID: 18566595. DOI: 10.1038/nri2343

14 Romano M, Fanelli G, Albany CJ, Giganti G and Lombardi G: Past, present, and future of regulatory T cell therapy in transplantation and autoimmunity. Front Immunol *10*: 43, 2019. PMID: 30804926. DOI: 10.3389/fimmu.2019.00043

15 Lužnik Z, Anchouche S, Dana R and Yin J: Regulatory T cells in angiogenesis. J Immunol *205(10)*: 2557-2565, 2020. PMID: 33168598. DOI: 10.4049/jimmunol.2000574

16 Nosbaum A, Prevel N, Truong HA, Mehta P, Ettinger M, Scharschmidt TC, Ali NH, Pauli ML, Abbas AK and Rosenblum MD: Cutting edge: Regulatory T cells facilitate cutaneous wound healing. J Immunol *196(5)*: 2010-2014, 2016. PMID: 26826250. DOI: 10.4049/jimmunol.1502139

17 Inoue Y, Amano H and Asari Y: Roles of regulatory T cells in enhancement of angiogenesis in a sponge implantation model. Kitasato Med J *48*: 105-117, 2018.

18 Uematsu S, Matsumoto M, Takeda K and Akira S: Lipopolysaccharide-dependent prostaglandin E(2) production is regulated by the glutathione-dependent prostaglandin E(2) synthase gene induced by the Toll-like receptor 4/MyD88/NF-IL6 pathway. J Immunol *168(11)*: 5811-5816, 2002. PMID: 12023384. DOI: 10.4049/jimmunol.168.11.5811

19 Park K, Amano H, Ito Y, Kashiwagi S, Yamazaki Y, Takeda A, Shibuya M, Kitasato H and Majima M: Vascular endothelial growth factor receptor-1 (VEGFR-1) signaling enhances angiogenesis in a surgical sponge model. Biomed Pharmacother *78*: 140-149, 2016. PMID: 26898435. DOI: 10.1016/j.biopha.2016.01.005

20 DiPietro LA: Angiogenesis and wound repair: when enough is enough. J Leukoc Biol *100(5)*: 979-984, 2016. PMID: 27406995. DOI: 10.1189/jlb.4MR0316-102R

21 Yasukawa K, Okuno T and Yokomizo T: Eicosanoids in skin wound healing. Int J Mol Sci *21(22)*: 8435, 2020. PMID: 33182690. DOI: 10.3390/ijms21228435

22 Kamoshita E, Ikeda Y, Fujita M, Amano H, Oikawa A, Suzuki T, Ogawa Y, Yamashina S, Azuma S, Narumiya S, Unno N and Majima M: Recruitment of a prostaglandin E receptor subtype, EP3-expressing bone marrow cells is crucial in wound-induced angiogenesis. Am J Pathol *169(4)*: 1458-1472, 2006. PMID: 17003499. DOI: 10.2353/ajpath.2006.051358

23 Samuelsson B, Morgenstern R and Jakobsson PJ: Membrane prostaglandin E synthase-1: a novel therapeutic target. Pharmacol Rev *59(3)*: 207-224, 2007. PMID: 17878511. DOI: 10.1124/pr.59.3.1

24 Fairweather M, Heit YI, Buie J, Rosenberg LM, Briggs A, Orgill DP and Bertagnolli MM: Celecoxib inhibits early cutaneous wound healing. J Surg Res *194(2)*: 717-724, 2015. PMID: 25588948. DOI: 10.1016/j.jss.2014.12.026

25 Iwanaga K, Okada M, Murata T, Hori M and Ozaki H: Prostaglandin E2 promotes wound-induced migration of intestinal subepithelial myofibroblasts *via* EP2, EP3, and EP4 prostanoid receptor activation. J Pharmacol Exp Ther *340(3)*: 604-611, 2012. PMID: 22138372. DOI: 10.1124/jpet.111.189845

26 Nishizawa N, Ito Y, Eshima K, Ohkubo H, Kojo K, Inoue T, Raouf J, Jakobsson PJ, Uematsu S, Akira S, Narumiya S, Watanabe M and Majima M: Inhibition of microsomal

prostaglandin E synthase-1 facilitates liver repair after hepatic injury in mice. J Hepatol *69(1)*: 110-120, 2018. PMID: 29458169. DOI: 10.1016/j.jhep.2018.02.009

27 Betto T, Amano H, Ito Y, Eshima K, Yoshida T, Matsui Y, Yamane S, Inoue T, Otaka F, Kobayashi K, Koizumi W, Shibuya M and Majima M: Vascular endothelial growth factor receptor 1 tyrosine kinase signaling facilitates healing of DSS-induced colitis by accumulation of Tregs in ulcer area. Biomed Pharmacother *111*: 131-141, 2019. PMID: 30579252. DOI: 10.1016/j.biopha.2018.12.021

28 Morimoto Y, Tamura R, Ohara K, Kosugi K, Oishi Y, Kuranari Y, Yoshida K and Toda M: Prognostic significance of VEGF receptors expression on the tumor cells in skull base chordoma. J Neurooncol *144(1)*: 65-77, 2019. PMID: 31240525. DOI: 10.1007/s11060-019-03221-z

29 Facciabene A, Peng X, Hagemann IS, Balint K, Barchetti A, Wang LP, Gimotty PA, Gilks CB, Lal P, Zhang L and Coukos G: Tumour hypoxia promotes tolerance and angiogenesis *via* CCL28 and T(reg) cells. Nature *475(7355)*: 226-230, 2011. PMID: 21753853. DOI: 10.1038/nature10169

30 Gupta S, Joshi K, Wig JD and Arora SK: Intratumoral FOXP3 expression in infiltrating breast carcinoma: Its association with clinicopathologic parameters and angiogenesis. Acta Oncol *46(6)*: 792-797, 2007. PMID: 17653902. DOI: 10.1080/02841860701233443

31 Okizaki S, Ito Y, Hosono K, Oba K, Ohkubo H, Kojo K, Nishizawa N, Shibuya M, Shichiri M and Majima M: Vascular endothelial growth factor receptor Type 1 signaling prevents delayed wound healing in diabetes by attenuating the production of IL-1β by recruited macrophages. Am J Pathol *186(6)*: 1481-1498, 2016. PMID: 27085138. DOI: 10.1016/j.ajpath.2016.02.014

32 Wang XQ, Zhou WJ, Luo XZ, Tao Y and Li DJ: Synergistic effect of regulatory T cells and proinflammatory cytokines in angiogenesis in the endometriotic milieu. Hum Reprod *32(6)*: 1304-1317, 2017. PMID: 28383711. DOI: 10.1093/humrep/dex067

Received June 23, 2022
Revised July 18, 2022
Accepted July 19, 2022